JOURNAL OF GEOPHYSICAL RESEARCH, VOL. 90, NO. C6, PAGES 11,945–11,948, NOVEMBER 20, 1985

A Simple Model of Estuarine Subtidal Fluctuations Forced by Local and Remote Wind Stress

RICHARD W. GARVINE

College of Marine Studies, University of Delaware, Newark

Observations of estuarine low subtidal sea level and current fluctuations have often shown domination by the remote effects of the wind, acting on the adjacent coastal ocean, over the local surface stress, acting on the estuary itself. The remote effects are transmitted to the estuary by impressment on its mouth of sea level change induced by the onshore component of coastal Ekman transport and become increasingly dominant as the frequency decreases. A simple, barotropic model is developed to investigate the joint action of these two wind forcing mechanisms. The relative shortness of most estuaries relative to low subtidal estuarine wavelengths explains the dominance of the remote effect for both sea level and barotropic current fluctuations in the estuary. For the same reason, however, surface slope is dominated by local wind setup. For an estuary with axis nearly parallel to the coast the two effects will operate either in concert or in opposition, depending on hemisphere and orientation of the estuary axis relative to the coast. For the geometries of both Chesapeake Bay and the Delaware Estuary the model predicts opposition with the remote effect dominant at lower frequencies, consistent with recent observations.

1. INTRODUCTION

Within the past decade, observations of subtidal sea level and current fluctuations in estuaries have revealed a dual nature to forcing by wind, its local or direct action upon the estuary surface, and its remote or indirect action over the adjacent shelf through the coastal Ekman effect in producing sea level fluctuations impressed on the estuary mouth. *Smith* [1977] found that the lagoonal estuary of Corpus Christi Bay sustained energetic sea level fluctuations that were coherent with cross-shore winds parallel to the bay inlet for short periods (2–4 days), consistent with local forcing, but coherent with alongshore winds, consistent with coastal Ekman setup, for longer periods. In similar geomorphology, *Wong and Wilson* [1984] found that spatially coherent subtidal sea level fluctuations in Great South Bay, Long Island, were forced primarily by alongshore winds through the coastal Ekman effect. For both Corpus Christi and Great South bays the wind-forced subtidal volume exchange with the adjacent shelf well exceeded the corresponding tidal exchange.

Similar responses have been reported for larger estuaries. *Wang and Elliott* [1978] found that in Chesapeake Bay, response to wind forcing at high subtidal frequencies, 2–4 days, was largely coherent with the local along-estuary wind stress, while at lower frequencies, 5–20 days, it was coherent with alongshore winds over the adjacent shelf. As a result of the estuary and coastal geometry, the remote mechanism even produced currents which flowed against the local wind within the estuary. *Wong and Garvine* [1984] found that the remote effect of the wind was dominant within the Delaware Estuary for all subtidal frequencies with energetic, barotropic currents flowing against the local wind, as in Chesapeake Bay for low frequencies. These currents were as large as those associated with the estuarine gravitational circulation.

At still larger scales, *Holbrook et al.* [1980] found that subtidal currents in the Strait of Juan de Fuca, a fjordlike estuary, were highly coherent with alongshore winds at the coast, but only weakly coherent with local, along-strait winds. The response was essentially baroclinic with downwelling (southerly) coastal winds driving a surface inflow and bottom outflow and upwelling (northerly) winds the reverse. Subsequently, *Klinck et al.* [1981] were able to demonstrate the generality of such responses to remote wind forcing for fjordlike estuaries by employing a two-layer, linear, frictionless model of the coupled ocean/estuary circulation.

The dominance of the remote wind forcing mechanism in the Delaware Estuary is clearly depicted in Figure 1, reproduced from *Wong and Garvine* [1984]. Low-pass filtered wind stress is plotted along with filtered currents obtained from 40-day-long current meter records at three depths on a mooring. The estuarine gravitational circulation shows clearly in the differences between the mean values at the three depths, the surface mean southward (seaward), the middepth nearly zero, and the bottom northward (landward). In addition, however, nearly barotropic subtidal fluctuations of about equal strength, 5–10 cm/s, are apparent. Several wind events occurred, the strongest from the north during October 22–26. In all of those with appreciable north/south components (along the estuary axis) the current change was opposite the wind, i.e., contrary to the local action of wind stress, but consistent with the action of sea level changes at the mouth that were induced by the coastal Ekman effect. In other words, the remote mechanism dominated the local one, as in Chesapeake Bay for low frequencies.

Two important questions thus arise from observations to date. What is the primary dynamical reason for the dominance of the remote wind forcing mechanism over the local for low subtidal frequencies? Are there circumstances of estuarine geometry, such as axis orientation relative to the local coastline and estuarine length, which control the degree of this dominance and determine whether the remote and local effects act in opposition to each other or in concert? To address these questions, I develop a simple, linear, barotropic model of wind-forced, low subtidal frequency motion that includes both the local and remote mechanisms. While not directly applicable to such highly stratified estuaries as the Strait of Juan de Fuca, the model should provide a conceptual explanation of the relative strengths of the local and remote wind forcing mechanisms for producing barotropic current and sea level fluctuations in estuaries such as Chesapeake Bay.

Paper number 5C0613.
0148-0227/85/005C-0613$05.00

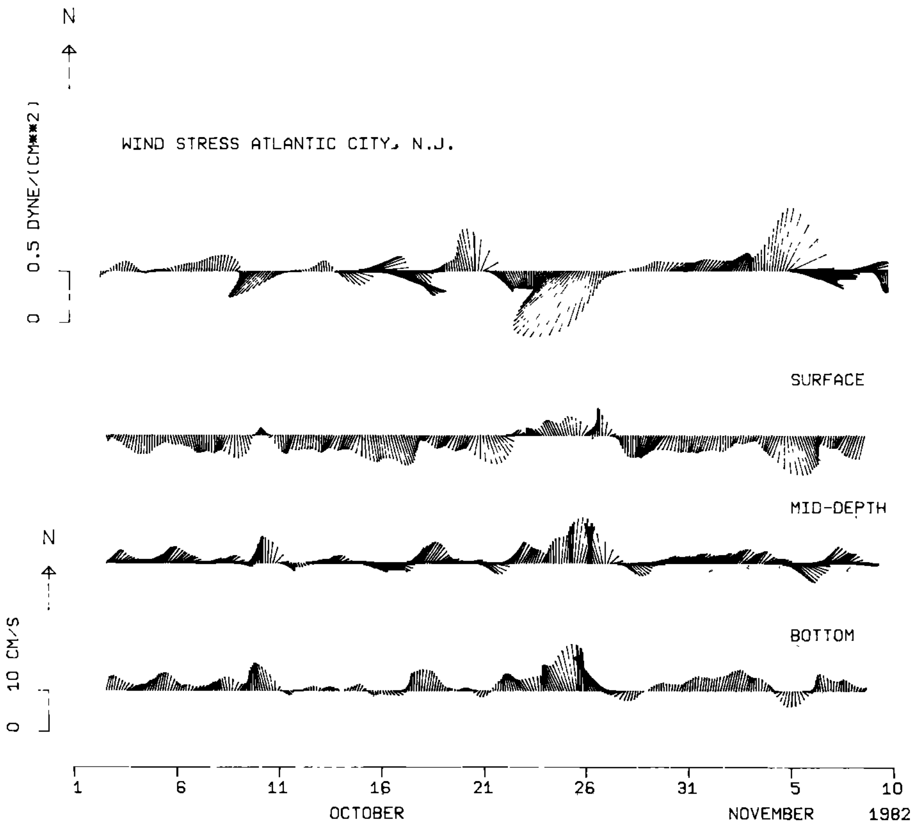

Fig. 1. Time series vector plots of low-pass filtered wind stress at Atlantic City, New Jersey, and current in the Delaware Estuary at three depths from a current meter mooring in 9 *m* of water. Vectors are drawn toward the direction of motion. North (upward on the figure) is nearly landward along the estuary locally. Wind stress and current magnitude scales are shown on the left. From *Wong and Garvine* [1984].

2. MODEL DEVELOPMENT

Figure 2 shows the model geometry in plan view. The estuary is a straight, rectangular channel of constant breadth b and constant depth h. Distance x^* along the estuary axis is measured from the mouth with a rigid barrier at $x^* = L^*$ representing the head. (Asterisks denote dimensional variables.) The direction of the coast is θ_c, measured counterclockwise from x^*.

Wind stress $\boldsymbol{\tau}_w$ drives the model. Here I take $\boldsymbol{\tau}_w$ to be uniform in space, since for the low frequencies of interest the atmospheric synoptic scale systems that produce it are typically much larger than the estuary and adjacent coastal ocean. Rectilinear, harmonic wind stress fluctuations are imposed with frequency ω, representative of the synoptic scale:

$$\boldsymbol{\tau}_w = \tau \mathbf{i}_\theta e^{i\omega t^*} \tag{1}$$

where $\tau \equiv |\boldsymbol{\tau}_w|$ and $\mathbf{i}_\theta$ is a unit vector in the direction the wind blows, i.e., at angle θ from x^* (Figure 2), and t^* is time. Typically, $\omega \sim 10^{-5}\ s^{-1}$ (7-day period), so that the resulting motion will be of low subtidal frequency, i.e., $\omega \ll 4\pi\ \mathrm{d}^{-1}$. Subsequently, all variables are understood to refer to such low subtidal, barotropic variations only.

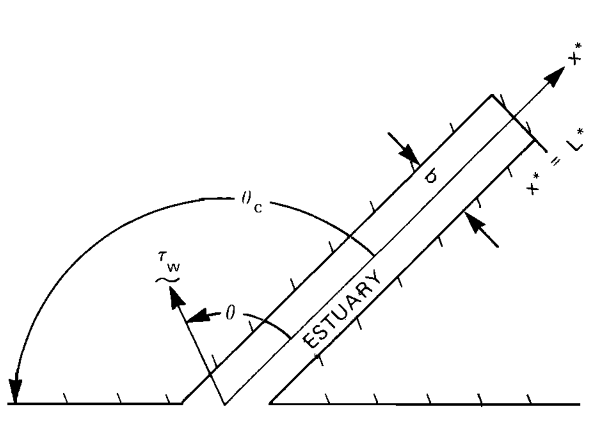

Fig. 2. Plan view of the model geometry.

Wind forcing enters the model in two ways, however, first, through $\tau_w^{(x)}$, the local wind stress acting along the estuary axis, and, second, through the remote action of the wind over the adjacent shelf by the production of cross-shelf surface Ekman flux and resulting coastal sea level change. I represent this remote forcing in the model through a boundary condition on the subtidal sea level η^* at the mouth as

$$\eta^*(0,t^*) = \alpha E \tag{2}$$

where $E \equiv (\tau/f) \cos(\theta - \theta_c)e^{i\omega t^*}$, the cross-shelf component of the Ekman flux, with f the Coriolis parameter. For simplicity, I take α, given empirically, to be real and positive; thus there will be no phase lag between the alongshore wind stress and coastal sea level. From subtidal coastal sea level records [e.g., *Wong and Garvine*, 1984] one finds that typically α is about $5 \times 10^{-3}\ \mathrm{cm^3\ dyn^{-1}\ s^{-1}}$.

The governing equations for the subtidal sea level in the estuary have the standard form

$$\frac{\partial u^*}{\partial t^*} = -g\frac{\partial \eta^*}{\partial x^*} + \frac{\tau_w^{(x)} - \tau_b^{(x)}}{\rho h} \quad (3a)$$

$$\frac{\partial u^*}{\partial x^*} = -\frac{1}{h}\frac{\partial \eta^*}{\partial t^*} \quad (3b)$$

where u^* is the vertically averaged or barotropic subtidal current, ρ is density, g the acceleration of gravity, and $\tau_b^{(x)}$ the bottom stress along x^*. Equation (3*a*) omits density gradient induced baroclinic pressure gradient, since it contributes little to the vertically averaged current fluctuations, as well as Coriolis effects, since the Kelvin number $bf/(gh)^{1/2}$ is assumed small, and advection of momentum, since η/h is assumed small, also. I represent the bottom stress by the common linear form

$$\tau_b^{(x)} = \rho C_D u_T u^*$$

where $C_D \sim 10^{-3}$ is a drag coefficient and u_T the root mean square tidal current, both constants.

Scaled variables are now introduced:

$$x \equiv (\omega/c)x^* \qquad L \equiv (\omega/c)L^* \qquad t \equiv \omega t^*$$

$$\eta \equiv \eta^*/a \qquad u \equiv hu^*/(ac)$$

Here $c = (gh)^{1/2}$, the long wave phase speed, and a is the standard deviation of the subtidal sea level. The scaled variables will be of order unity, in general. Using them, equations (3) simplify to

$$\frac{\partial u}{\partial t} + \frac{\partial \eta}{\partial x} + \lambda u = W \cos \theta e^{it} \quad (4a)$$

$$\frac{\partial u}{\partial x} + \frac{\partial \eta}{\partial t} = 0 \quad (4b)$$

where two constants appear, $W \equiv \tau/(\rho\omega ca)$, a dimensionless local wind parameter, and $\lambda \equiv c_D u_T/(h\omega)$, a dimensionless bottom friction parameter. The sea level scale a is generally set by the coastal sea level response and is about 50 cm for an alongshore wind stress of 1 dyn/cm^2 (see, for example, *Wong and Garvine*, [1984, Figure 10]). Thus, with $\omega = 10^{-5}$ s^{-1} again and $c = 10$ m/s (or $h \simeq 10$ m), one finds $W = 2$, i.e., W is of order unity. Similarly, λ is typically order unity. The boundary conditions now have the form

$$\eta(0,t) = A(0)e^{it} \quad (5a)$$

$$u(L,t) = 0 \quad (5b)$$

where $A(0) \equiv \alpha\tau/(af) \cos(\theta - \theta_c)$, the scaled sea level amplitude at the mouth.

3. MODEL SOLUTION

Equations (4) are readily solved with the aid of the waveforms

$$\eta = A(x)e^{it} \qquad u = U(x)e^{it} \quad (6)$$

From (4*b*) we have $A = iU'$ (where prime denotes d/dx) which, used in (4*a*), gives

$$U'' + (1 - i\lambda)U = -iW \cos \theta \quad (7)$$

The solution of (7), subject to (5) is

$$U(x) = \frac{i}{K^2 \cosh KL}[A(0)K \sinh\{K(L - x)\} + W \cos \theta(\cosh KL - \cosh Kx)] \quad (8a)$$

so that

$$A(x) = \frac{1}{K \cosh KL}[A(0)K \cosh\{K(L - x)\} + W \cos \theta \sinh Kx] \quad (8b)$$

where K is a complex wave number of order unity given by

$$K \equiv (-1 + i\lambda)^{1/2} = [(r - 1)/2]^{1/2} + i[(r + 1)/2]^{1/2}$$

where $r \equiv (1 + \lambda^2)^{1/2}$, a real number.

4. SOLUTION FOR L SMALL

Because of the complex nature of K and the frequent appearance of hyperbolic functions, the solutions in (8) fail to provide ready insight into estuarine wind forced subtidal fluctuations. In particular, while the remote and local wind forcing mechanisms are clearly separated and tagged by the coefficients $A(0)$ and W, respectively, these solutions, as written, are silent as to which mechanism is dominant. One might even conclude, erroneously, that the two mechanisms have equal strength, since $A(0)$ and W are both $O(1)$. One can, nevertheless, put the solutions in a clear form by first recognizing the small size of L (and thus x) and then expanding all the hyperbolic functions in L or x.

From its definition we have $L = (\omega/c)L^*$. Thus, if $\omega = 10^{-5}$ s^{-1}, $c = 10$ m/s (h about 10 m), and $L^* = 100$ km, $L = 0.1$. In physical terms then, most estuaries are short when forced at low subtidal frequencies and become increasingly shorter as the frequency decreases. In dimensional terms, disturbances, having phase speed c, traverse the estuary length L^* many times in a period $2\pi/\omega$. Equivalently, the dimensional wavelength of these disturbances $2\pi c/\omega$ is very long compared to L^*, so that the boundary condition at the head is felt strongly throughout. We can anticipate, then, that phase differences in η between head and mouth will be small, analogous to a Helmholtz accoustical resonator. In contrast, at tidal frequencies ω will be an order of magnitude larger, so that $L \sim 1$ then, permitting large phase differences. Recognition of the shortness of estuaries at low subtidal frequencies is the main point of this paper. As will be clear next, this shortness dictates the dominance of the remote wind forcing mechanism over the local one for both sea level and current barotropic fluctuations.

After expanding U and A in (8) in series for small x and L and taking the real part of the waveforms (6) one finds through $O(L)$;

$$u(x, t) = -(L - x)[A(0) + 1/2W \cos \theta(L + x) + O(L^2)] \sin t \quad (9a)$$

$$\eta(x,t) = [A(0) + (W \cos \theta)x + O(L^2)] \cos t \quad (9b)$$

$$\partial\eta/\partial x = W \cos \theta \cos t + A(0)(L - x)(\cos t + \lambda \sin t) + O(L^2) \quad (9c)$$

These solutions show clearly the following physical characteristics of estuarine, wind forced, barotropic, subtidal motion.

1. Both sea level and barotropic current variations are produced dominantly by the remote wind effect; the local effect is smaller by $O(L)$. In contrast, the surface slope $\partial\eta/\partial x$ is dominantly produced by the local wind. Both these results follow directly from the shortness of the estuary relative to low subtidal wavelengths. To lowest order, sea level in the estuary merely follows with no phase lag that at the mouth produced by the longshore wind stress through the coastal

Ekman effect, while the current responds as constrained by mass continuity to fill or empty the estuary as required. Sea level variations within the estuary on the wavelength scale, $2\pi c/\omega$ dimensionally, are slight because L^* is much shorter; thus the primary contributor to surface slope is local wind setup, as (9c) shows.

2. The contribution to sea level and barotropic current variations by the local wind effect increases linearly with distance from the mouth, however. Consequently, longer estuaries, such as Chesapeake Bay, will exhibit greater local effects than shorter ones, especially near the head, but even such longer ones will show dominance of the remote effect, especially in their seaward reaches. These characteristics were indeed found in sea level records for Chesapeake Bay by *Wang and Elliott* [1978].

3. Sea level and current are in quadrature phase through $O(L)$ with current leading. Consequently, the corresponding Stokes current, proportional to the time average of the product $u\eta$ over a period [*Lonquet-Higgins*, 1969], is everywhere zero. The quadrature phase follows from the standing wave character of the response, a consequence again of the short length. To lowest order the surface slope is in phase with the local wind stress and either in phase or of opposite phase with sea level.

4. Bottom friction, manifest in (9) by the parameter λ, is effective only on the surface slope and, then, only at $O(L)$. The response is thus predominantly inviscid.

5. The barotropic current u will be of $O(L)$ rather than $O(1)$, as (1a) indicates. This reduction from that anticipated by the initial scaling is also a result of the shortness of the estuary. The proper scale for the dimensional current u^* is thus $L \cdot ac/h = a\omega L^*/h$. Indeed, this scaling may be derived directly from the continuity equation (3b) if we now take $\partial/\partial x^* \sim 1/L^*$ rather than ω/c as used before. For $a = 0.5$ m, $\omega = 10^{-5}$ s^{-1}, $L^* = 100$ km, and $h = 10$ m, for example, this gives a scale of 5 cm/s, roughly the amplitude shown for the current fluctuations in Figure 1.

Retention in the model of arbitrary angle θ_c between the estuary axis and the coastline (Figure 2) permits an assessment of the degree to which this geometry affects the combined action of the two mechanisms, remote and local. For $|\theta_c| \approx 90°$ the two mechanisms operate nearly independently, since the remote effect, as always, will be proportional to the alongshore component, while the local effect will be proportional then only to the onshore component. For θ_c near either 0° or 180°, i.e., when the estuary axis nearly parallels the coast, both effects will be proportional to the alongshore component largely and thus will act either in concert or in opposition. For θ_c small they will be in concert in the northern hemisphere but in opposition in the southern. For θ_c nearly 180° the reverse is true. The Delaware Estuary and Chesapeake Bay, for example, both illustrate the latter, since they have $\theta_c \approx 160°$. *Wang and Elliott*'s [1978] results for Chesapeake Bay and *Wong and Garvine*'s [1984] for the Delaware Estuary exhibit this opposition clearly. Since the remote effect is dominant, the barotropic current flows against the local wind, as in the wind events shown in Figure 1 for the Delaware.

Wind-forced, low subtidal frequency barotropic fluctuations in an estuary will, in general, be dominated by the remote rather than the local effect because of the relative shortness of most estuaries compared to the scale of the low subtidal wavelength. Recognition of this dominance and its causes, illustrated here by a simple model, should aid in the better design of estuarine observations and numerical models.

Acknowledgment. This work was supported by the Physical Oceanography Program of the National Science Foundation under grant OCE-8315207.

REFERENCES

Holbrook, J. R., R. D. Muench, and G. A. Cannon, Seasonal observations of low frequency atmospheric forcing in the Strait of Juan de Fuca, in *Fjord Oceanography*, edited by H. J. Freeland, D. M. Farmer and C. D. Levings, Eds., pp. 305–318, Plenum, New York, 1980.

Klinck, J. M., J. J. O'Brien, and H. Svendsen, A simple model of fjord and coastal circulation interaction, *J. Phys. Oceanogr.*, *11*, 1612–1626, 1981.

Longuet-Higgins, M. S., On the transport of mass by time-varying ocean currents. *Deep Sea Res.*, *16*, 431–447, 1969.

Smith, N. P., Meteorological and tidal exchanges between Corpus Christi Bay, Texas, and the northwestern Gulf of Mexico, *Estuarine Coastal Mar. Sci.*, *5*, 511–520, 1977.

Wang, D.-P., and A. J. Elliott, Nontidal variability in the Chesapeake Bay and Potomac River: Evidence for nonlocal forcing, *J. Phys. Oceanogr.*, *8*, 225–232, 1978.

Wong, K.-C., and R. W. Garvine, Observations of wind-induced, subtidal variability in the Delaware Estuary, *J. Geophys. Res.*, *89*, 10,589–10,598, 1984.

Wong, K.-C., and R. E. Wilson, Observations of low frequency variability in Great South Bay and relations to atmospheric forcing, *J. Phys. Oceanogr.*, *14*, 1893–1900, 1984.

R. W. Garvine, College of Marine Studies, University of Delaware, Robinson Hall, Newark, DE 19716.

(Received June 27, 1985;
accepted July 22, 1985.)